IEEE Access
Multidisciplinary | Rapid Review | Open Access Journal

Received November 4, 2018, accepted November 28, 2018, date of publication January 3, 2019, date of current version January 23, 2019.

Digital Object Identifier 10.1109/ACCESS.2018.2887252

A Reliability Prediction Methodology for LED Arrays

BO SUN[1], JIAJIE FAN[2], (Senior Member, IEEE), XUEJUN FAN[3], (Fellow, IEEE), GUOQI ZHANG[4], (Fellow, IEEE), AND GUOHAO ZHANG[1]

[1]Faculty of Information Engineering, Guangdong University of Technology, Guangzhou 510006, China
[2]College of Mechanical and Electrical Engineering, Hohai University, Changzhou 213022, China
[3]Department of Mechanical Engineering, Lamar University, Beaumont, TX 77710, USA
[4]Department of Microelectronics, Delft University of Technology, 2628 CD Delft, The Netherlands

Corresponding author: Bo Sun (bosun@gdut.edu.cn)

ABSTRACT In this paper, a physics of failure-based prediction method is combined with statistical models to consider the impact of current crowding and current droop effects on the reliability of LED arrays. Electronic-thermal models of LEDs are utilized to obtain the operation conditions under the influences of current crowding and current droop. A Markov chain-based model is used to calculate the probability distribution of each failure mode, including the lumen decay and catastrophic failure. Two types of LEDs were selected for a numerical study. The proposed prediction method provides the realistic reliability prediction results. It is found that the properties of LEDs have a great impact on their hazard rates of LED arrays. The equivalent resistance, third-order non-radiative coefficient, and radiative coefficient of LEDs are critical to the reliability of an LED array.

INDEX TERMS Catastrophic failure, electronic-thermal model, LED array, Markov chain, reliability prediction.

NOTATIONS

$X(t)$	Probability distribution of a system;
x_i	Probability of State i;
P	Transition matrix of an LED array;
n	Number of LED strings in parallel;
m	Number of LEDs in series;
$h_{i\to j}$	Probability of State i transfers to State j in Δt;
h_s	Hazard rate of an LED string;
λ_0	LED's basic hazard rate;
T_A	Ambient temperature;
E_a	LED's activation energy;
T_j	LED's junction temperature;
P_{th}	LED's thermal power;
R_{th}	LED's thermal resistance;
P_{LED}	LED's input power;
P_{Ra}	LED's radiative power;
$\eta(I)$	Efficiency of LED with Current I;
$V_f(I)$	Forward voltage of LED with Current I;
$I(i)$	Current of LED in State i;
R_s	Equivalent resistance;
V_0	Zero-current voltage;
η_0	Basic efficiency;
A_e	1st order non-radiative coefficient;
B_e	Radiative coefficient;
C_e	3rd order non-radiative coefficient;
I_a	Total input current of the array;
$\varphi(i)$	Relative radiative power of the array in State i;

I. INTRODUCTION

Degradations including lumen depreciation and color shift, are usually considered as major failure modes of LEDs. The LED's lifetime refers to the time at which an LED's lumen maintenance degrades to 70% [1]–[3]. Many reliability prediction methods for solid state lighting [4]–[8] focus on LEDs' degradations. In recent years, many novel technologies have been applied to produce more reliable LEDs. For example, the ultraviolet LEDs have attracted more and more research concern [9], [10]. The under-etching process and glass substrate technology has been developed for GaN-based LEDs [11], [12]. ZnO nano-particles has been used to enhance performance and lifetime of white-light LEDs [13]. Meanwhile, many advanced packaging methods have developed to extend LED's lifetime. For instance, reliable phosphor materials for white-light LEDs have been studied [14]–[17]. Thin film structure and silicon substrate have been used to reduce LEDs' thermal resistance [18], [19].

Graphene have been implemented by LED packaging [20], [21]. Remote phosphor technologies have been utilized for LED lamps [22]. Optimization approaches of LED packages have been developed [23], [24]. Via these new technologies, the effect of lumen depreciation has been highly reduced. In 2013, it has reported that the lumen depreciation of an LED lamp is less than 3% after 25000 hours' operation [25]. Currently, LED often has a lifetime as long as 25,000 hours [2], [26]. If such trend continues, it is reasonable to believe that the lumen depreciation could be reduced to an insignificant level in future solid state lighting products.

Beside the lumen depreciation with aging time, LED's catastrophic failure, which will result in zero light output and open circuit [27], [28], is seen as one of major failures. In many area lighting applications, the light source is an LED array with many strings. Although the current balancing techniques have been developed [29], mainstream applications still connect paralleled LED strings directly. When one of LEDs is failed, the entire string is disconnect from the array. The current in the remaining strings will redistribute, leading current crowding and current droop. The current crowding effect will bring a higher forward voltage and thus more input power [30]. The current droop will cause a decrease of power efficiency [31]. Under inferences of these two effects, the LED array will produce more heat and have an elevated junction temperature and thus higher failure rate [32], [33]. Due to the large number of LEDs, the reliability test for an LED array is expensive and time-consuming. Conventional system reliability models [33] usually suppose that the failure rate of each LED stay at a constant value. Such an assumption may result significant errors in reliability assessment of LED arrays. It is necessary to develop a reliability prediction approach with consideration of failure rate changing caused by current crowding and current droop for LED arrays.

In this work, a physics of failure-based prediction methodology is combined with statistical models to consider the impact of LED's catastrophic failure, current crowding and current droop effects on of reliability LED arrays. Electronic-thermal models of LEDs are utilized to obtain conditions of each operation status under influences of current crowding and current droop. LED's catastrophic failure, current crowding and current droop depend on current operation status, but are independent of the history of operation conditions. The probability degradation of an LED array can consider as a Markov process. Thus, a Markov chain-base model is used to calculate the probability distribution of each operation status based on operation conditions.

This paper is organized as follows. Section II describes the proposed reliability model of LED arrays based on the Markov Chain. In Section III, physics-based models of LED are described. Experiments and model parameter extractions are introduced in Section IV. In Section V, two types of LED are analyzed to predict reliability of an LED array via the proposed methodology. Section VI concludes this work finally.

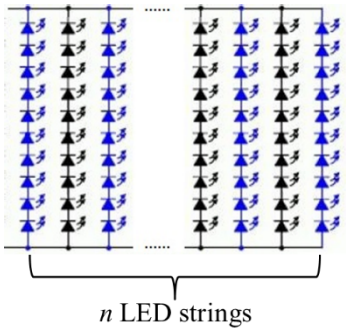

FIGURE 1. A typical LED array structure.

II. RELIABILITY MODEL OF LED ARRAY

Figure 1 shows a typical LED array. Supposes that the array consists of n LED strings in parallel, each string has m identical LEDs. The driving current distributes evenly in all working LED strings. Each string has the same operation conditions and thus the hazard rate. The catastrophic failure of each LED will be considered, which will lead an open circuit [34].

For a system has n+1 operation states, probability distribution at time t can be denoted as a set $X(t)$ [35]:

$$X(t) = [x_0(t), x_1(t)...x_n(t)] \tag{1}$$

As discussed in previous works [36], [37], an electronic system with catastrophic failures can be described by the Markov Chain. Probability variations of the system at time $t + \Delta t$ can be obtained by the following equation [35]:

$$dX(t)/dt = X(t) \cdot P \tag{2}$$

where P is system's transition matrix:

$$P = \begin{bmatrix} h_{0\to 0} & h_{0\to 1} & \cdots & h_{0\to n} \\ h_{1\to 0} & h_{1\to 1} & \cdots & h_{1\to n} \\ \vdots & \vdots & \ddots & \vdots \\ h_{n\to 0} & h_{n\to 1} & \cdots & h_{n\to n} \end{bmatrix} \tag{3}$$

where $h_{i\to j}$ means the probability of State i transfers to State j. In this work, the overall catastrophic failure of an LED is considered. State x represents that the array has x failed strings. Since the overall probability of the array stays unchanged, thus for any certain i:

$$\sum_{j=0}^{n} h_{i\to j} = 0 \tag{4}$$

The catastrophic failure of the selected LED is unrecoverable, hence for any $i \geq j$:

$$h_{i\to j} = 0 \tag{5}$$

Therefore, the transition matrix P degrades to:

$$P = \begin{bmatrix} h_{0\to 0} & h_{0\to 1} & \cdots & h_{0\to n} \\ 0 & h_{1\to 1} & \cdots & h_{1\to n} \\ \vdots & \vdots & \ddots & \vdots \\ 0 & 0 & \cdots & h_{n\to n} \end{bmatrix} \tag{6}$$

In the case of $i = j$, $h_{i\to j}$ can be obtained by Eq. (4). For any $i \le j$, $h_{i\to j}$ in the transition matrix can be obtained by the following equation [38]:

$$h_{i\to j} = C_{n-i}^{j-i} \cdot h_s^{i-j}(i) = \frac{(n-i)!}{(n-j)! \cdot (i-j)!} h_s^{i-j}(i) \tag{7}$$

where the hazard rate of each LED string h_s depends on LEDs' physics-based models which will be discussed in the following section.

III. PHYSICS-BASED MODELS OF LED

For an LED string with m LEDs, $h_s(i)$ can be obtained by [33]:

$$h_s(i) = m \cdot \lambda_0 \cdot e^{\frac{E_a}{\kappa}[\frac{1}{T_j(i)} - \frac{1}{T_A}]} \tag{8}$$

where, λ_0 is the basic hazard rate at the ambient temperature T_A, E_a is the activation energy of the selected LED, T_j is the LED's junction temperature. In this work, λ_0 and E_a are obtained from the empirical models [33], and T_j can be calculated by LEDs' thermal model.

The interactions of the junction temperature of chips within a package are not significant [39]. Thus, module-level thermal interactions between LEDs may be neglected. Once the LED reaches thermal equilibrium point, the junction temperature T_j are functions of the component's thermal power P_{th} [40]:

$$T_j = P_{th} \cdot R_{th} + T_A \tag{9}$$

where, R_{th} is the thermal resistance of the LED. In this work, R_{th} can be from data-sheet or experiments of the selected LEDs. Without consideration of the lumen depreciation, the P_{th} can be obtained by:

$$P_{th} = P_{LED} - P_{Ra} = P_{LED} \cdot [1 - \eta(i)] \tag{10}$$

where $\eta(I)$ is LED's efficiency at current I, P_{Ra} is the radiative power of each LED which equals to product of P_{LED} and $\eta(I)$, P_{LED} is the input power:

$$P_{LED}(I) = V_f(I) \cdot I \tag{11}$$

For ideal diodes, forward voltage $V_f(I)$ can be determined by the following equation [30]:

$$I = I_s \cdot [e^{V_f(I)/V_T} - 1] \tag{12}$$

For LED in high-current status, $V_f(I)$ is approximately proportional to driving current I [30]:

$$V_f(I) = R_s \cdot I + V_0 \tag{13}$$

where V_0 can be seemed as zero-current forward voltage, R_s is equivalent resistance of the LED.

Theoretically, $\eta(I)$ is determined by both temperature droop and current droop [31], [41]. In comparison with the current droop, the temperature droop becomes negligible. Hence, the $\eta(I)$ can be described the following function:

$$\eta(I) = \eta_0 \frac{B_e I}{A_e + B_e I + C_e I^2} \tag{14}$$

where η_0 is basic efficiency, A_e and C_e are the 1st and 3rd order non-radiative power factor, B_e is the radiative power factor. These current droop related parameters are dependent on material and structure properties of the LED, and will be extracted experimentally in the Section IV.

As mentioned before, a current redistribution will be caused by the catastrophic failure. Failure of any of the m LEDs in the string will lead an open circuit of the entire string. Therefore, current of each working LED string is a function of number of failed LED strings i:

$$I(i) = I_a/(n-i) \tag{15}$$

where I_a is the input current of the entire LED array which usually keeps at a constant value. Therefore, P_LED, $V_f(I)$ and η_I) are also function of number of failed strings i. This work uses the relative radiative power $\varphi(i)$ as failure criteria, which is approximately proportional to lumen maintenance of the entire LED array. According to Eq.(10) to (14), $\varphi(i)$ can be calculated by:

$$\varphi(i) = \frac{m \cdot (n-i) \cdot P_{LED}(i) \cdot \eta(i)}{m \cdot n \cdot P_{LED}(i) \cdot \eta_0} = \frac{V_f(i) \cdot \eta(i)}{V_f(0) \cdot \eta(0)} \tag{16}$$

As discussion above, the basic hazard rate λ_0 and the activation energy E_a will be obtained from the empirical models [33]. Other parameters, including LEDs' thermal resistance, parameters of LED's power and efficiency, will be extracted experimentally in the following section.

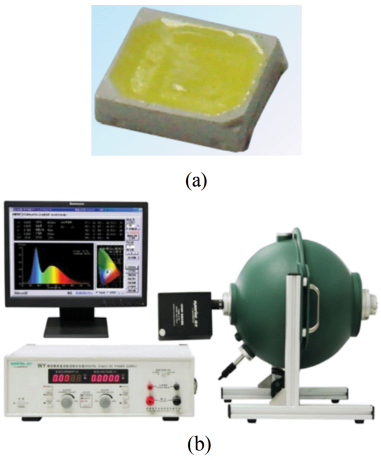

FIGURE 2. (a) The selected LED package and (b) test plat-from.

IV. EXPERIMENT AND PARAMETER EXTRACTION

This work selects a common-used type of LED package [42], as shown in Figure 2 (a). Two types of LED chips, LED A and B, which have different current and temperature sensitivities, were integrated into the selected LED package. The rated current and CCT of selected LEDs are 20mA and 6000K. Input power of LED A and B are around 56mW and 51mW.

In order to determine to determine R_S, V_0, η_0, A_e, B_e and C_e, two groups of samples were tested in five current levels, from 20mA to 100mA. Simple size of every

group is 15. Each sample was placed on a thermal plate inside a 50cm integrating sphere system as shown in Figure 2 (b). Then, the electronic and optical characteristics of each sample, including current, forward voltage, radiant power and efficiency, are measured at different conditions. For each current level, the temperature of each sample sweeps from 303K to 343K.

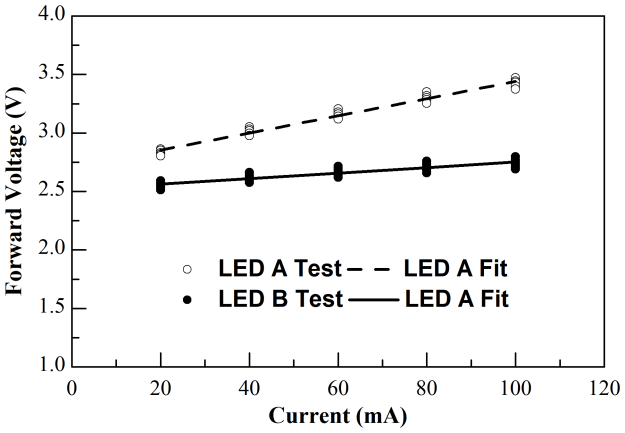

FIGURE 3. Voltage curves vs. driving current.

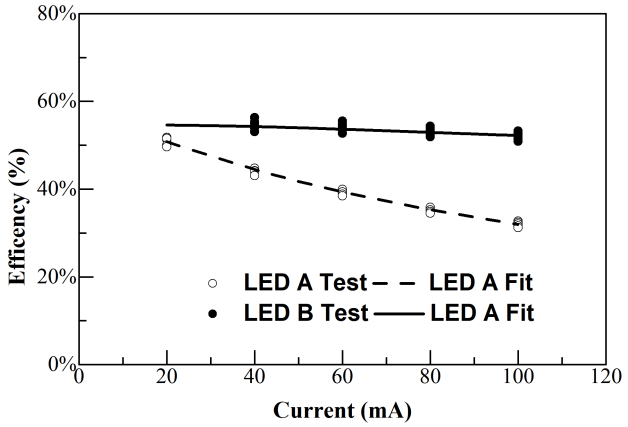

FIGURE 4. Efficiency curves vs. driving current.

Figure 3 displays the forward voltage curves as functions of driving current. The forward voltage curves increase linearly with each driving current. For each certain current, variations of V_f in different temperatures are less than 0.2V. Therefore, V_f is primarily determined by the driving current. Figure 4 shows the efficiency curves as functions of driving current. The power efficiency curves decrease with each driving current. For each certain current, variations of V_f in different temperatures are less than 3%. As a result, the T-droop can be neglected in this work. Then, the measured forward voltage curves were fitted by Eq.(13), whereas the efficiency curves were fitted by Eq.(14) by the least square method, obtaining parameters of the LED models. Table 1 summarizes the averaged values of the model parameters. Goodness of fit for $V_f(I)$ and $\eta(I)$ are larger than 0.85. Therefore, fitting curves have good agreements with tested results.

In order to determine the thermal resistance R_{th} of the selected LED packages experimentally, the same group of samples were tested in room temperature (300K) by the T3ster system. The junction temperature increments $T_j - T_A$ were measured in different current levels, from 20mA to 100mA. The thermal power can be obtained from Eq.(10).

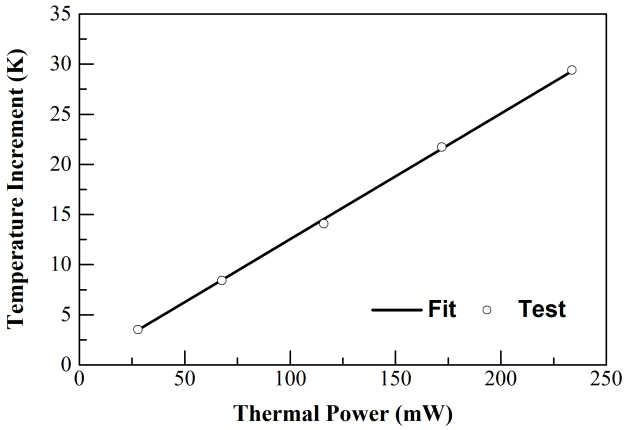

FIGURE 5. Temperature increment vs. thermal power.

TABLE 1. Parameters of LED models.

Parameters	LED A	LED A
R_S	7.352 ohm	2.354 ohm
V_0	2.681 V	2.516 V
η_0	59.58%	56.69%
A_e	0	1.087×10^{-1}
B_e	1.900×10^{-1}	2.529×10^{-1}
C_e	1.642×10^{-3}	2.075×10^{-4}
R_{th}	125.9K·W^{-1}	125.9K·W^{-1}

Figure 5 gives the temperature increment as a function of thermal power. Then, the measured junction temperature increments were fitted by Eq.(9) by the least square method, the average value of R_{th} can be obtained. As shown in Figure 4, R_{th} of the selected LED is about 125.9 $K \cdot W^{-1}$. The R^2 value of R_{th} fitting is larger than 0.99. Thus, the thermal model has a good agreement with tested results.

V. CASE STUDIES AND RESULTS

The proposed approach provides a general methodology for an LED array with considerations of current distribution and hazard rate changing. A 7 by 10 LED array (7 LED strings, 10 LEDs per string) has been selected. An ideal constant current power supply provides driving current to the LED array. Since junction temperatures and driving current of LEDs will change with the number of failed LED strings, the actual hazard rate and radiative power of LEDs will be different from the pre-selected values. The LED is pre-selected with the activation energy and pre-factor of $E_{\alpha,\beta} = 0.45eV$ and $\lambda_0 = 2.74 \times 10^{-6}$ (T_A=300K), according to the empirical models [33]. The other parameters that appear in Eq. (8) to (14) are listed in Table 1. The relative radiative power is used as the failure criterion. If the relative radiative power drops below 70% of its initial value, lumen maintenance

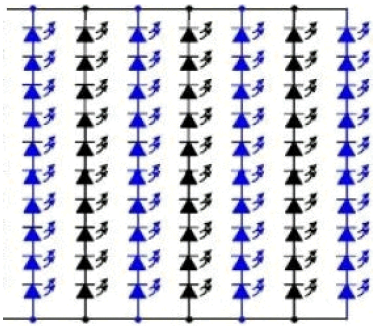

FIGURE 6. The selected LED array.

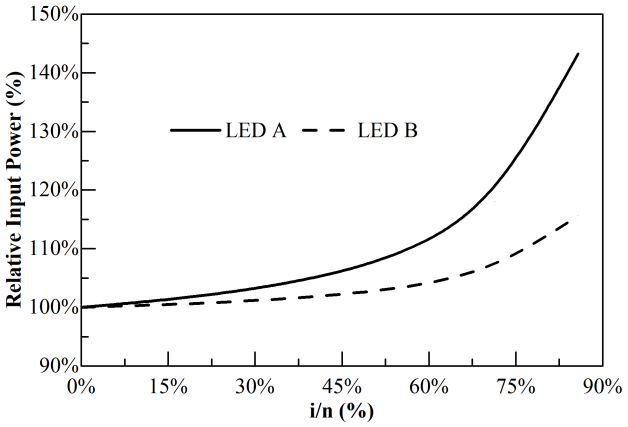

FIGURE 7. Relative input power.

may degrade below 70%, the entire LED array is considered failed. The catastrophic failure, which refers to all LED strings failed, can be seemed as a special case, owing that the radiative power drops to zero. The details of the results will be discussed below.

As explained in Eq.(13), the current crowding lead by a reduction of working LED strings will bring a higher forward voltage of each LED. Since the total current of the entire array keeps unchanged, input power of the array will be increased. Figure 7 displays the relative input power of the entire LED array as a function of i/n ratio. The input power of the LED array increases exponentially with the i/n ratio. At $i/n = 6/7$, the array relative input power with LED A and B increase about 43% and 15%. According to Eq. (11) and (13), increment of input power is approximately proportional to R_s.

Figure 8 displays the relative radiative power of the entire LED array as a function of i/n ratio. The relative radiative power of LED A (Solid Line) decreases to about 65% when the i=6, leading lumen decay of the entire array. Meanwhile, for the LED B, the relative radiative power (Dash Line) increases about 3%. The current droop effect has little impact on LED B. The relative radiative power of the LED array will be always larger than 70% in the selected current range.

Due to the effects of current crowding and current droop, input power and thermal power will increase if several LED strings failed, leading a higher LED's junction temperature. Figure 8 displays the LED's junction temperature as a function of i/n ratio. The junction temperature of each LED

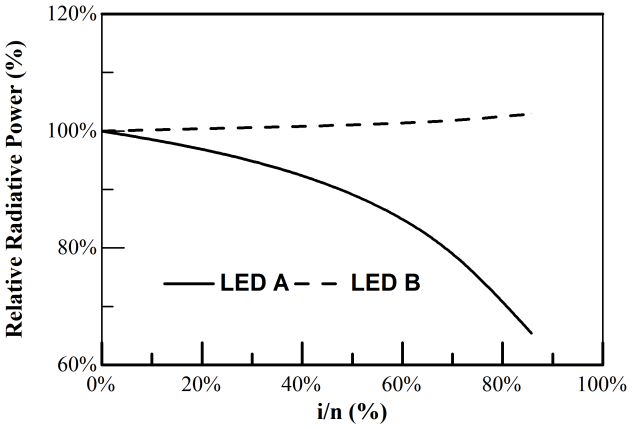

FIGURE 8. Relative radiative power.

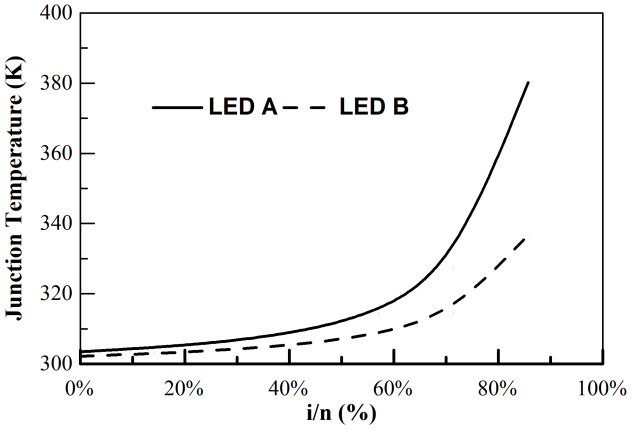

FIGURE 9. Junction temperature curves.

increases exponentially with the number of failed LED strings. When only one of 7 LED strings works, the junction temperature of LED A and B rise to about 380K and 336K respectively.

The elevated junction temperatures will cause a higher hazard rate of each LED string. Figure 9 displays hazard rates of LED strings as a function of i/n ratio. When the junction temperature of LED A and B rise to about 380K and 336K, their hazard rates increase to about 1.249×10^{-3} and 2.086×10^{-4} respectively. Properties of LEDs have great impact on their hazard rates, the constant hazard rate assumption may bring significant prediction differences.

In Figure 10, cumulated failure rates of both LEDs are illustrated. The failure probability curves rise exponentially with time. In about 20000 hours, failure probabilities increase to about 33.0% and 8.5% for LED A and B respectively. Moreover, consideration of LED's properties is critical to reliability prediction of LED arrays. LEDs with better overdriving capability can compose a more reliable LED array. Therefore, the proposed prediction method, which considers electronic and thermal characteristic of LEDs, may provide a realistic prediction results of an LED array.

Then, a numerical study has been carried out to investigate impacts of model parameters on the LED array's failure

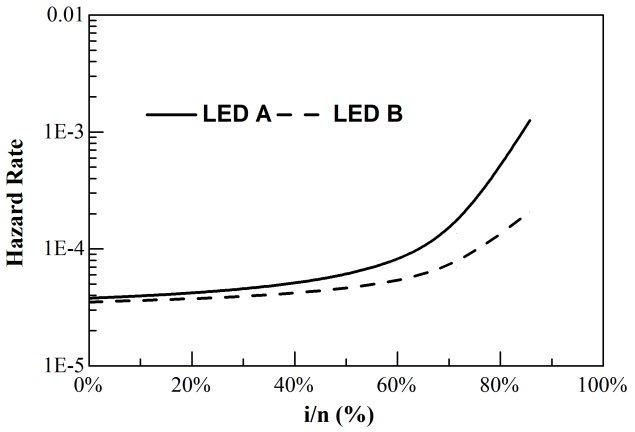

FIGURE 10. Hazard rates of LED strings.

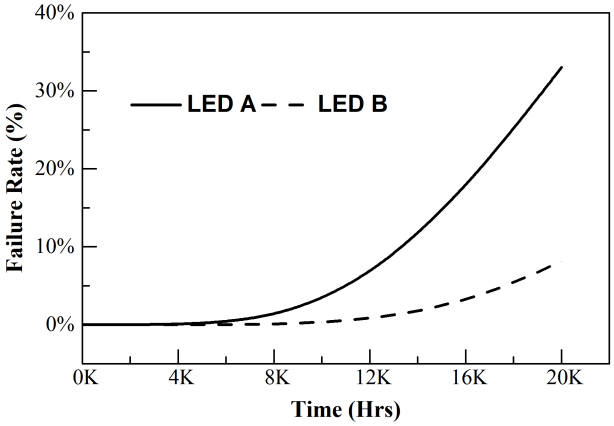

FIGURE 11. Cumulated failure rates of the LED array.

TABLE 2. Failure probability prediction results.

Parameters	Failure Probability	% of differences
V_0	42.88%	9.85%
C_e	35.24%	2.21%
R_S	34.67%	1.65%
B_e	30.97%	-2.05%
η_0	26.25%	-6.78%

probability, including R_s, V_0, η_0, A_e, B_e and C_e. Firstly, each parameter has increased 20% respectively. Table 2 lists failure probability prediction results.

Parameter B_e and η_0 have negative effects on the LED array's failure probability. Because increments of these two parameters will reduce thermal power of each LED. Conversely, increasing of Parameter C_e will produce more heat. Hence, it has a positive effect on the array's failure probability. Similarly, higher Parameter R_s and V_0 will bring higher input power, leading a higher junction temperature. As a result, these two parameters have a positive effect on the array's failure probability either.

Secondly, parameters of LED A will be replaced by relevant ones of LED B respectively, to study their contributions to differences between LED A and B. Table 3 gives the simulation results.

TABLE 3. Numerical study results.

Replaced Parameter	$\varphi(6)$	Failure probability	% of contributions
η_0	65.5%	34.8%	-7.07%
A_e	65.5%	33.3%	-1.16%
V_0	66.8%	29.8%	13.01%
R_S	52.4%	27.5%	22.05%
B_e	73.9%	26.4%	26.67%
C_e	121.2%	13.6%	78.28%
R_S and C_e	97.0%	8.91%	97.05%
R_S, B_e and C_e	100.7%	8.24%	99.74%

As shown in Table 3, Parameter C_e significantly affects the relative radiative power and failure probability of the LED array. If Parameter C_e drops from 1.642×10^{-3} to 2.075×10^{-4}, the radiative power will always increase with the number of failed LED strings, and array's failure probability decreases from 33.0% to 13.6%. It contributes about 78% of the differences between LED A and B. Parameter C_e and R_s have combined effects on the failure probability. Replacement of these two parameters contributes about 97.1% of the differences between LED A and B. However, owing to less input power, a less R_s value brings less radiative power. As shown in Table 3, if the R_s value is decreased from 7.352 to 2.354, the $\varphi(6)$ value will reduce from 65.5% to 52.4% ($C_e = 1.642 \times 10^{-3}$), or from 121.2% to 97.0% ($C_e = 2.075 \times 10^{-4}$). Because of the weaken current droop effect, the rise of Parameter B_e partly cancels the influence of Parameter R_s on $\varphi(6)$, and enhances the impact of Parameter C_e and R_s on the failure probability. The combination of LED B's B_e, C_e and R_s contributes more than 99.7% of the differences between LED A and B. In conclusion, as shown in the numerical study, Parameter B_e, C_e and R_s have significant impact on reliability of an LED array. Consideration of these parameters may provide a more realistic reliability prediction result.

VI. CONCLUSION

In this work, a physics-based prediction methodology is combined with statistical models to consider the impact of current crowding and current droop effects on of reliability LED arrays. Electronic-thermal models of LEDs are utilized to obtain conditions of each operation status under the influences of LED's catastrophic failure, current crowding and current droop. Based on operation conditions, a Markov chain-base model is used to calculate the probability distribution of each operation status, including the lumen decay and catastrophic failure. A 7×10 LED array and two types of LEDs have been selected for case studies. Finally, a numerical study has been carried out to investigate impacts of model parameters on the LED array's reliability.

For LED A, when 6 of the 7 strings failed, relative input power increases about 43%, relative radiative power decreases to about 65%, junction temperature and hazard rate rise to 380K and 1.249×10^{-3} respectively. In 20000 hours, failure probability of the array is 33.0%. For LED B, when 6 of the 7 strings failed, relative input power and relative radiative power increase about 15% and 3% respectively junction temperature rises to 336K and hazard rate rises

to 2.086×10^{-4}. In 20000 hours, failure probability of the array is 8.2%. For the numerical study, if C_e drops from 1.642×10^{-3} to 2.075×10^{-4}, the radiative power will always increase with the number of failed LED strings, and array's failure probability decreases from 33.0% to 13.6%. The combination of LED B's B_e, C_e and R_s contributes more than 99.7% of the differences between LED A and B.

The proposed prediction method provides more realistic prediction results of an LED arrays. It has been found that the properties of LEDs have great impact on their hazard rates. Among LED's parameters, the 3rd order non-radiative coefficient C_e, equivalent resistance R_s and radiative coefficient B_e have significant impact on reliability of the selected LED array.

REFERENCES

[1] C. Qian, J. Fan, X. Fan, and G. Zhang, "Prediction of lumen depreciation and color shift for phosphor-converted white light-emitting diodes based on a spectral power distribution analysis method," *IEEE Access*, vol. 5, pp. 24054–24061, 2017.

[2] W. D. V. Driel, X. Fan, and G. Q. Zhang, *Solid State Lighting Reliability Part 2*. Cham, Switzerland: Springer, 2018.

[3] K. Lu, W. Zhang, and B. Sun, "Multidimensional data-driven life prediction method for white LEDs based on BP-NN and improved-Adaboost algorithm," *IEEE Access*, vol. 5, pp. 21660–21668, 2017.

[4] J. Fan, M. G. Mohamed, C. Qian, X. Fan, G. Zhang, and M. Pecht, "Color shift failure prediction for phosphor-converted white LEDs by modeling features of spectral power distribution with a nonlinear filter approach," *Materials*, vol. 10, no. 7, p. 819, 2017.

[5] J. Fan, C. Qian, X. Fan, G. Zhang, and M. Pecht, "*In-situ* monitoring and anomaly detection for LED packages using a Mahalanobis distance approach," in *Proc. 1st Int. Conf. Rel. Syst. Eng. (ICRSE)*, Oct. 2015, pp. 1–6.

[6] J. Fan, C. Qian, X. Fan, G. Q. Zhang, and M. Pecht, "Fault diagnostics and lifetime prognostics for phosphor-converted white LED packages," in *Solid State Lighting Reliability Part 2*. Cham, Switzerland: Springer, 2018, pp. 255–299.

[7] J. Fan, C. Qian, K.-C. Yung, X. Fan, G. Zhang, and M. Pecht, "Optimal design of life testing for high-brightness white LEDs using the six sigma DMAIC approach," *IEEE Trans. Device Mater. Rel.*, vol. 15, no. 4, pp. 576–587, Dec. 2015.

[8] J. Fan, K.-C. Yung, and M. Pecht, "Prognostics of lumen maintenance for high power white light emitting diodes using a nonlinear filter-based approach," *Rel. Eng. Syst. Saf.*, vol. 123, pp. 63–72, Mar. 2014.

[9] L. Liu *et al.*, "High-detectivity ultraviolet photodetectors based on laterally mesoporous GaN," *Nanoscale*, vol. 9, no. 24, pp. 8142–8148, 2017.

[10] H. Hu, S. Zhou, X. Liu, Y. Gao, C. Gui, and S. Liu, "Effects of GaN/AlGaN/Sputtered AlN nucleation layers on performance of GaN-based ultraviolet light-emitting diodes," *Sci. Rep.*, vol. 7, Mar. 2017, Art. no. 44627.

[11] C. Zheng, J. Lv, S. Zhou, and S. Liu, "Improvement of luster consistency between the p-Pad and the n-Pad of GaN-based light-emitting diodes via the under-etching process," *J. Korean Phys. Soc.*, vol. 70, no. 8, pp. 765–770, 2017.

[12] P. An *et al.*, "Growth and optical properties of gallium nitride film on glass substrates," *Phys. Status Solidi C*, vol. 13, nos. 5–6, pp. 200–204, 2016.

[13] L. Liu, X. Tan, D. Teng, M. Wu, and G. Wang, "Simultaneously enhancing the angular-color uniformity, luminous efficiency, and reliability of white light-emitting diodes by ZnO@SiO_2 modified silicones," *IEEE Trans. Compon., Packag., Manuf. Technol.*, vol. 5, no. 5, pp. 599–605, May 2015.

[14] H. Xu *et al.*, "Crystal structure and luminescence properties of the blue-green-emitting $Ba_9(Lu, Y)_2Si_6O_{24}$:Ce^{3+} phosphor," *Luminescence*, vol. 32, no. 5, pp. 812–816, 2017.

[15] W. Lu *et al.*, "Tunable white light of a Ce^{3+},Tb^{3+},Mn^{2+} triply doped $Na_2Ca_3Si_2O_8$ phosphor for high colour-rendering white LED applications: Tunable luminescence and energy transfer," *Dalton Trans.*, vol. 46, no. 28, pp. 9272–9279, 2017.

[16] Y. Liu *et al.*, "An excellent cyan-emitting orthosilicate phosphor for NUV-pumped white LED application," *J. Mater. Chem. C*, vol. 5, no. 47, pp. 12365–12377, 2017.

[17] H. Xu *et al.*, "Luminescence and energy transfer of color-tunable $Na_6Ca_3Si_6O_{18}$:Ce^{3+},Tb^{3+} phosphors for WLED," *Opt. Laser Technol.*, vol. 89, pp. 151–155, Mar. 2017.

[18] H. T. Chen, Y. F. Cheung, H. W. Choi, S. C. Tan, and S. Y. Hui, "Reduction of thermal resistance and optical power loss using thin-film light-emitting diode (LED) structure," *IEEE Trans. Ind. Electron.*, vol. 62, no. 11, pp. 6925–6933, Nov. 2015.

[19] X. Liu, Z. Lv, and S. Liu, "Low thermal-resistance silicon-based substrate for light-emitting diode packaging," *IEEE Trans. Compon., Packag., Manuf. Technol.*, vol. 5, no. 10, pp. 1387–1392, Oct. 2015.

[20] F. Zhu, Y. Kan, K. Tang, and S. Liu, "Investigation of thermal properties of Ni-coated graphene nanoribbons based on molecular dynamics methods," *J. Electron. Mater.*, vol. 46, no. 8, pp. 4733–4739, 2017.

[21] K. Duan, F. Zhu, K. Tang, L. He, Y. Chen, and S. Liu, "Effects of chirality and number of graphene layers on the mechanical properties of graphene-embedded copper nanocomposites," *Comput. Mater. Sci.*, vol. 117, pp. 294–299, May 2016.

[22] X. Yu, B. Xie, Q. Chen, Y. Ma, R. Wu, and X. Luo, "Thermal remote phosphor coating for phosphor-converted white-light-emitting diodes," *IEEE Trans. Compon., Packag., Manuf. Technol.*, vol. 5, no. 9, pp. 1253–1257, Sep. 2015.

[23] H.-Y. Tang, H.-Y. Ye, X.-P. Chen, C. Qian, X.-J. Fan, and G.-Q. Zhang, "Numerical thermal analysis and optimization of multi-chip LED module using response surface methodology and genetic algorithm," *IEEE Access*, vol. 5, pp. 16459–16468, 2017.

[24] J. P. Kim and S. W. Jeon, "Investigation of light extraction by refractive index of an encapsulant, a package structure, and phosphor," *IEEE Trans. Compon., Packag., Manuf. Technol.*, vol. 6, no. 12, pp. 1815–1819, Dec. 2016.

[25] *Lumen Maintenance Testing of the Philips 60-Watt Replacement Lamp L Prize Entry*, U.S. Dept. Energy, Washington, DC, USA, Jul. 2013.

[26] W. D. van Driel and X. J. Fan, *Solid State Lighting Reliability: Components to Systems*, vol. 1. Cham, Switzerland: Springer Science and Business Media, Springer, 2012.

[27] B. Sun, X. Jiang, K.-C. Yung, J. Fan, and M. G. Pecht, "A review of prognostic techniques for high-power white LEDs," *IEEE Trans. Power Electron.*, vol. 32, no. 8, pp. 6338–6362, Aug. 2017.

[28] M.-H. Chang, D. Das, P. V. Varde, and M. Pecht, "Light emitting diodes reliability review," *Microelectron. Rel.*, vol. 52, no. 5, pp. 762–782, May 2012.

[29] R. Zhang and H. S.-H. Chung, "Paralleled LED strings: An overview of current-balancing techniques," *IEEE Ind. Electron. Mag.*, vol. 9, no. 2, pp. 17–23, Jun. 2015.

[30] E. F. Schubert, T. Gessmann, and J. K. Kim, *Light Emitting Diodes*. Hoboken, NJ, USA: Wiley, 2005.

[31] J. Piprek, "Efficiency droop in nitride-based light-emitting diodes," *Phys. Status Solidi A*, vol. 207, no. 10, pp. 2217–2225, 2010.

[32] L. Liu, L. Yin, D. Teng, J. Zhang, X. Ma, and G. Wang, "An explanation for catastrophic failures of GaN-based vertical structure LEDs subjected to thermoelectric stressing," *J. Phys. D, Appl. Phys.*, vol. 48, no. 30, p. 305102, 2015.

[33] *MIL-HDBK-217F: Reliability Prediction of Electronic Equipment*, U.S. Dept. Defense, Arlington, VA, USA, 1991.

[34] R. Wu, F. Blaabjerg, H. Wang, and M. Liserre, "Overview of catastrophic failures of freewheeling diodes in power electronic circuits," *Microelectron. Rel.*, vol. 53, nos. 9–11, pp. 1788–1792, 2013.

[35] K. M. Ramachandran, "Appendix B—Review of Markov chains," in *Mathematical Statistics with Applications in R*, C. P. Tsokos, Ed., 2nd ed. Boston, MA, USA: Academic, 2015, pp. 737–741.

[36] A. Khosroshahi, M. Abapour, and M. Sabahi, "Reliability evaluation of conventional and interleaved DC-DC boost converters," *IEEE Trans. Power Electron.*, vol. 30, no. 10, pp. 5821–5828, Oct. 2015.

[37] B. Sun, X. Fan, W. Van Driel, C. Cui, and G. Zhang, "A stochastic process based reliability prediction method for LED driver," *Rel. Eng. Syst. Saf.*, vol. 178, pp. 140–146, Oct. 2018.

[38] C. W. Gardiner, *Handbook of Stochastic Methods*, vol. 3. Berlin, Germany: Springer, 1985.

[39] X. J. Fan, "Development, validation, and application of thermal modeling for a MCM power package," in *Proc. 19th Annu. IEEE Semiconductor Therm. Meas. Manage. Symp.*, Mar. 2003, pp. 144–150.

[40] B. Sun *et al.*, "A novel lifetime prediction for integrated LED lamps by electronic-thermal simulation," *Rel. Eng. Syst. Safety*, vol. 163, pp. 14–21, Jul. 2017.
[41] D. S. Meyaard *et al.*, "Temperature dependent efficiency droop in GaInN light-emitting diodes with different current densities," *Appl. Phys. Lett.*, vol. 100, no. 8, p. 081106, 2012.
[42] *Specification of HL-A-2835H489W-S1-08L-HR3 LED PLCC-2 Package*, Honglitronic, Beijing, China, 2014.

BO SUN received the B.S. degree in microelectronics from the South China University of Technology, Guangzhou, China, in 2008, the M.S. degree in electrical engineering from Lamar University, Beaumont, TX, USA, in 2011, and the Ph.D. in electrical engineering from the Delft University of Technology, Delft, The Netherlands, in 2017.

Since 2012, he has been a Reliability Engineer with the State Key Laboratory of Solid-State Lighting, China. He is currently a Researcher with the School of Information Engineering, Guangdong University of Technology. His current research interests include the reliability and failure analysis of RF and mm-wave device and package and the lifetime prediction of photo-electronic devices and systems.

JIAJIE FAN (M'14–SM'17) received the B.S. degree in inorganic materials science and engineering from the Nanjing University of Technology, Nanjing, China, in 2006, the M.S. degree in material science and engineering from the East China University of Science and Technology, Shanghai, China, in 2009, and the Ph.D. degree in industrial and systems engineering from The Hong Kong Polytechnic University, Hong Kong, in 2014. He is currently an Associate Professor with the College of Mechanical and Electrical Engineering, Hohai University, Changzhou, Jiangsu, China. He is also a Post-Doctoral Research Fellow with the Delft University of Technology (Beijing Research Centre), and the State Key Laboratory of Solid-State Lighting, China. His main research interests include reliability assessment for LEDs, prognostics and health management for LED lightings, failure diagnosis and prognosis for electric devices and system, and advanced microelectronic packaging and assembly. He is a Senior Member of the IEEE. He is an Associate Editor of the IEEE Access and a Register of certified Six Sigma Green Belt at the Hong Kong Society for Quality.

XUEJUN FAN (SM'06–F'19) received the B.S. and M.S. degrees in applied mechanics from Tianjin University, Tianjin, China, in 1984 and 1986, respectively, and the Ph.D. degree in solid mechanics from Tsinghua University, Beijing, China, in 1989.

He was a Member of Technical Staff and the Group Leader of the Institute of Microelectronics, Singapore, from 1997 to 2000, a Senior Member Research Staff with the Philips Research Lab, Briarcliff Manor, NY, USA, from 2001 to 2004, and a Senior Staff Engineer with Intel Cooperation, Chandler, AZ, USA, from 2004 to 2007. In his earlier career, he was promoted to Full Professor, at the age of 27, at the Taiyuan University of Technology, Shanxi, China, in 1991, and became one of the youngest full professors in China at that time. He is currently a Professor with the Department of Mechanical Engineering, Lamar University, Beaumont, TX, USA, and also a Visiting Professor with the State Key Laboratory of Solid-State Lighting, China. His current research interests include the areas of design, modeling, material characterization, and reliability in micro-/nano-electronic packaging and microsystems.

He has published over 180 technical papers, several book chapters, and three books. He holds several patents. He received the IEEE CPMT Exceptional Technical Achievement Award, in 2011, and the Best Paper Award of the IEEE Transactions on Components and Packaging Technologies, in 2009. He is an IEEE CPMT Distinguished Lecturer.

GUOQI ZHANG (M'03–F'14) received the Ph.D. degree in aerospace engineering from the Delft University of Technology, Delft, The Netherlands, in 1993.

He was with Philips as a Principal Scientist, from 1994 to 1996, the Technology Domain Manager, from 1996 to 2005, the Senior Director of Technology Strategy, from 2005 to 2009, and the Philips Fellow, from 2009 to 2013. He was a Professor with the Technical University of Eindhoven, from 2002 to 2005, and a Chair Professor with the Delft University of Technology, from 2005 to 2013. Since 2013, he has been a Chair Professor with the Department of Microelectronics, Delft University of Technology. His research focuses on heterogeneous micro-/nano-electronics packaging, system integration, and reliability.

He has published more than 350 papers, including more than 140 journal papers, three books, and 17 book chapters. He holds more than 100 patents. He was elected as an IEEE Fellow, in 2014. He received the Outstanding Contributions to Reliability Research by the European Center for Micro/Nanoreliability, Berlin, in 2007, the Excellent Leadership Award from EuroSimE, the Special Achievement Award from ICEPT, and the IEEE CPMT Outstanding Sustained Technical Contribution Award, in 2015. He is one of pioneers in developing More than Moore strategy when he served as the Chair of MtM Technology Team, European's Nanoelectronics Platform, in 2005.

GUOHAO ZHANG received the B.S. and M.D. degree in electromagnetics theory and microwave technology from Southeast University, Nanjing, China, in 1985 and 1988, respectively, and the Ph.D. degree in micro-electronics from the University of Leeds, U.K., in 1996.

He was a Senior Engineer with Epsilon Lambda Electronics Corporation, from 1996 to 1998, and a Principal Engineer with California Amplifier, Inc., from 1998 to 2004. From 2004 to 2012, he was with Skyworks Solutions Inc., as a Senior Engineering Manager and a Senior Principal Engineer. Since 2012, he has been serving as the Dean of the School of Information Engineering and the Director of the RFIC Lab, Guangdong University of Technology. He has focused on the development and commercialization of power amplifier (PA), LNA, antenna switch, and RF front-end module for wireless communication application. He has contributed over 30 papers. He holds over 20 patents, authorized or pending. Throughout his career, his research interests are in RF/analog mixed-signal integrated circuits in deep submicrometer CMOS and heterostructure silicon–germanium bipolar transistors. He received the Skyworks' 2008 Innovation Award for developing a novel PA structure for modern smart phones.